

Annealing effect on temperature stability and mechanical stress at the “ $\text{Cd}_x\text{Pb}_{1-x}\text{S}$ film — substrate” interface

L. N. Maskaeva^{ab*}, A. D. Kutyavina^a, A. V. Pozdin^a,
 B. N. Miroshnikov^c, I. N. Miroshnikova^c, V. F. Markov^{ab}

^a Ural Federal University,

19 Mira st., Ekaterinburg, 620002, Russia

^b Ural Institute of the State Fire Service of the EMERCOM of Russia

22 Mira st., Ekaterinburg, 620022, Russia

^c National Research University “Moscow Power Engineering Institute”

14 Krasnokazarmennaya st., Moscow, 111250, Russia

*email: larisamaskaeva@yandex.ru

Abstract. The article establishes the upper temperature steadiness limit of $\text{Cd}_x\text{Pb}_{1-x}\text{S}$ supersaturated solid solutions obtained by chemical bath deposition. $\text{Cd}_x\text{Pb}_{1-x}\text{S}$ ($x = 0.06$; 0.122; 0.176) and ($x = 0.02$ –0.05) films remained stable under the heating up to 405–410 and 450 K, respectively. SEM studies have shown that heating of $\text{Cd}_x\text{Pb}_{1-x}\text{S}$ films ($x = 0.02$ –0.05) to 620 K leads to the structure destruction. Internal mechanical compressive stresses at the “ $\text{Cd}_x\text{Pb}_{1-x}\text{S}$ film-substrate” interface was calculated in the range of 300–900 K for the first time ever, the highest values reached 2000–2750 kN/m² for a number of the films compositions. In contrast to solid solutions, the expansion stresses up to 100 kN/m² were derived for the CdS layer at 900 K. The obtained temperature steadiness boundaries and the mechanical stresses of $\text{Cd}_x\text{Pb}_{1-x}\text{S}$ films must be taken into account in the development of photonic devices based on such materials.

Keywords: chemical bath deposition (CBD); thin films; $\text{Cd}_x\text{Pb}_{1-x}\text{S}$ solid solutions; annealing; mechanical stress

Received: 12.10.2020. Accepted: 27.12.2020. Published: 30.12.2020.

© Maskaeva L. N., Kutyavina A. D., Pozdin A. V., Miroshnikov B. N.,
 Miroshnikova I. N., Markov V. F., 2020

Introduction

One of the most important places among photosensitive semiconductor compounds is occupied by $\text{Cd}_x\text{Pb}_{1-x}\text{S}$ substitutional solid solutions, which are used to register visible and infrared radiation in the range of 0.4–3.0 μm . The most common areas of their practical use are the manufacture of IR detectors [1, 2], environmental control devices [3, 4], solar cells [5–7], as well as fast-response flame detectors [8].

The most effective method for the synthesis of films of $\text{Cd}_x\text{Pb}_{1-x}\text{S}$ solid solutions is chemical deposition from aqueous media (chemical bath deposition CDB). During this process, layers are formed with a B1 structure that are strongly supersaturated with respect to the substituting component [9]. Expansion of the temperature range of using photonic devices based on $\text{Cd}_x\text{Pb}_{1-x}\text{S}$ films presupposes a clear

knowledge of the temperature boundaries of the solid solutions stability of various compositions, as well as their mechanical characteristics. Given the high level of supersaturation in chemically deposited films of $\text{Cd}_x\text{Pb}_{1-x}\text{S}$ solid solutions, a significant increase in temperature can lead to structural, morphological, and phase transformations in the layer [10], as well as the appearance of internal mechanical stresses at the “film — substrate” interface [11]. The reason of their occurrence is the difference in the values of the crystal lattice constants, elastic moduli, and thermal expansion coefficients of the film and substrate. Since the film and the substrate are rigidly connected to each other, and the film is much thinner than the substrate, it can experience significant mechanical stress of compression or tension to match the geometry of the substrate [11].

Even an approximate estimate of elastic stresses is important for practical application. It will make possible to qualitatively determine the distribution of stresses in a thin-film layer and evaluate their influence. Thus, annealing of ZnS and ZnSe films obtained by thermal discrete evaporation on NaCl cleavages, quartz and silicon substrates, has led, in particular, to the vanishing of inclusions of the high-temperature wurtzite phase in the sphalerite matrix, to improvement of the structure and homogenization of the phase composition. In this case, the films heating to 200 °C for an hour has caused to the appearance of mechanical stresses in the layers, reaching approximately $-170 \cdot 10^9 \text{ N/m}^2$ [12, 13]. Moreover, the authors of the works note

that the mechanical stresses in the films on the rock salt cleavage represent the expansion ones, and stresses in the films sedimented on quartz and silicon substrates are the compressive ones. It was shown in [14] that internal mechanical compressive stresses in ZnSe films chemically deposited at 353 K are proportional to an increase in their thickness and depend on the thermal expansion coefficients of the film and substrate. In this regard, it is necessary to take into account the compatibility of the thermal expansion coefficients of the used substrates and the semiconductor layer for creating multilayer functional structures.

In [15], we showed that the magnitude of the mechanical compressive stresses arising at the “film — substrate” interface are presumably related to various conditions of nucleation and growth during the chemical deposition of $\text{Cd}_x\text{Pb}_{1-x}\text{S}$ layers on silicon, siall, fused quartz, ITO, slide and porous glasses substrates. In this case, the magnitude of the internal elastic stresses in the layers is asymbatic to the temperature expansion coefficients for the studied substrate materials. At the same time, there are no data on temperature boundaries of stability and internal mechanical stresses in $\text{Cd}_x\text{Pb}_{1-x}\text{S}$ supersaturated solid solutions films.

Thereby, in this work, we intend to establish the effect of annealing on the temperature stability and mechanical stresses at the “ $\text{Cd}_x\text{Pb}_{1-x}\text{S}$ film — substrate” interface for various phase compositions of solid solutions.

Experimental

$\text{Cd}_x\text{Pb}_{1-x}\text{S}$ ($x \leq 0.176$) solid solutions films were obtained by chemical bath deposition from a reaction mixture contain-

ing fixed concentrations of sodium citrate $\text{Na}_3\text{C}_6\text{H}_5\text{O}_7$, an aqueous solution of ammonia NH_4OH , and thiourea $\text{N}_2\text{H}_4\text{CS}$.

The concentration of cadmium chloride CdCl_2 was varied from 0.01 to 0.1 mol/l. The content of lead acetate $\text{Pb}(\text{CH}_3\text{COO})_2$ was 0.04 and 0.06 mol/l. Deposition was carried out in sealed reactors on previously degreased sital substrates for 120 min in a TS-TB-10 thermostat at 353 K with an accuracy of maintaining the temperature of ± 0.1 K.

The thickness of the obtained films was estimated using an interference microscope (Linnik microinterferometer) MII-4M with a measurement error of 20%.

The degradation of the synthesized $\text{Cd}_x\text{Pb}_{1-x}\text{S}$ ($x = 0.06; 0.122; 0.176$) solid solutions was studied by isothermal annealing in an argon atmosphere in the temperature range 298–673 K for 1 hour in a SNOL 7,2|1100L muffle furnace. In parallel, the resistance of the $\text{Cd}_x\text{Pb}_{1-x}\text{S}$ films ($x = 0.02\text{--}0.05$) was continuously monitored at heating from 300 to 900 K in air (rate ~ 12 K/min), followed by slow cooling to room temperatures.

The crystal structure of synthesized $\text{Cd}_x\text{Pb}_{1-x}\text{S}$ solid solution films was studied by X-ray diffraction method using dif-

fractometer Dron-4 with copper anode $\text{Cu K}\alpha_{1,2}$.

The structural and morphological characteristics of the as-deposited $\text{Cd}_x\text{Pb}_{1-x}\text{S}$ films were studied using a MIRA 3 LMU scanning electron microscope at an electron beam accelerating voltage of 10 kV, and the annealed ones were investigated using a Vega II SBU scanning electron microscope (Tescan, Czech Republic) at an electron beam accelerating voltage of 20 kV.

An approximate estimate of the mechanical stresses $\sigma_{\Delta\alpha}$ in the “ $\text{Cd}_x\text{Pb}_{1-x}\text{S}$ solid solution film — substrate” two-layer structure was carried out according to the equation proposed in [16]:

$$\sigma_{\Delta\alpha} = \frac{6 \cdot E_{\text{Cd}_x\text{Pb}_{1-x}\text{S}} \cdot (\alpha_{\text{sub}} - \alpha_{\text{Cd}_x\text{Pb}_{1-x}\text{S}}) \cdot h_{\text{Cd}_x\text{Pb}_{1-x}\text{S}} \cdot \Delta T}{(1 - \nu_{\text{Cd}_x\text{Pb}_{1-x}\text{S}}) \cdot (3h_{\text{sub}} - 4h_{\text{Cd}_x\text{Pb}_{1-x}\text{S}})} \quad (1)$$

where $E_{\text{Cd}_x\text{Pb}_{1-x}\text{S}}$ — Young's modulus of $\text{Cd}_x\text{Pb}_{1-x}\text{S}$ solid solution; $\alpha_{\text{sub}}, \alpha_{\text{Cd}_x\text{Pb}_{1-x}\text{S}}$ — thermal expansion coefficient of sital substrate and film, respectively; ΔT — setpoint temperature difference; $\nu_{\text{Cd}_x\text{Pb}_{1-x}\text{S}}$ — film Poisson's ratio; $h_{\text{sub}}, h_{\text{Cd}_x\text{Pb}_{1-x}\text{S}}$ — thickness of substrate and films, respectively, upon condition $h_{\text{sub}} \gg h_{\text{Cd}_x\text{Pb}_{1-x}\text{S}}$.

Results and discussion

The effect of the annealing temperature on the content of the substituent component (cadmium sulfide) in $\text{Cd}_x\text{Pb}_{1-x}\text{S}$ solid solutions is shown in Fig. 1, which images the equilibrium phase diagram of the CdS–PbS system. $\text{Cd}_x\text{Pb}_{1-x}\text{S}$ films with initial CdS contents of 6.0, 12.2, and 17.6 mol.% were annealed at 403, 473, 573, and 673 K for 1 h. The layers were obtained from a reaction mixture containing 0.04 mol/l lead acetate with varying the cadmium chloride content from 0.02 to 0.1 mol/l.

Annealing for 1 hour at 673 K demonstrated almost complete correspond-

ence of the composition of the annealed films to the equilibrium phase diagram of the PbS–CdS system [17]. The obtained results confirm the supersaturated metastable character of the chemically deposited $\text{Cd}_x\text{Pb}_{1-x}\text{S}$ solid solutions films ($0.060 < x < 0.176$). XRD studies of the annealed layers have revealed that, all samples retain diffraction reflections corresponding to the B1 structure. However, they shift to the region of smaller angles, which means an increase in the lattice period of the solid solution. In addition, the background intensity increases due to the formation of an indi-

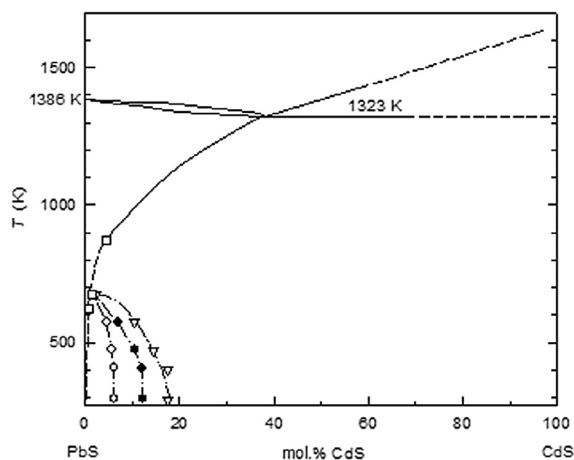


Fig. 1. Effect of the annealing temperature on the composition of $\text{Cd}_x\text{Pb}_{1-x}\text{S}$ supersaturated solid solutions in the range 403–673 K and correspondence of obtained data to the equilibrium phase diagram of the CdS — PbS system. Initial content of CdS in solid solution samples at 298 K, mol.%: 6.0 (○), 12.2 (●), 17.6 (▽) 17.6. The duration of the annealing was 1 hour. Phase equilibrium diagram of CdS — PbS is given according to [17], dash line denotes extrapolated data [17]

vidual X-ray amorphous phase of CdS. At the same time, no additional reflections were detected on the XRD patterns.

The established changes in the initial compositions of the $\text{Cd}_x\text{Pb}_{1-x}\text{S}$ supersaturated solid solutions are a consequence of their decomposition into two phases: a solid solution with a lower cadmium content (x) and an individual CdS phase.

The decay indicator of the studied solid solutions is also a changing their electrophysical properties. For this purpose, we investigated the dependence of the resistance R of $\text{Cd}_x\text{Pb}_{1-x}\text{S}$ films in the temperature range from 300 to 900 K (Fig. 2). Layers synthesized from a reaction mixture with a lead acetate concentration of 0.06 mol/l were used as initial samples. The initial content of cadmium chloride in the reactor was 0.01, 0.02, 0.04, 0.10 mol/l. According to the XRD data, the resulting films had the compositions: $\text{Cd}_{0.02}\text{Pb}_{0.98}\text{S}$, $\text{Cd}_{0.03}\text{Pb}_{0.97}\text{S}$, $\text{Cd}_{0.04}\text{Pb}_{0.96}\text{S}$ and $\text{Cd}_{0.05}\text{Pb}_{0.95}\text{S}$.

As seen from Fig. 2, as the temperature rises to 450 K, the films resistance decreases by about an order of magnitude. The behavior of the curves of all the films under discussion in the range of 300–450 K is approximately similar. However, a slightly greater resistance decrease is observed for the $\text{Cd}_{0.02}\text{Pb}_{0.98}\text{S}$ solid solution (1) compared to other samples. It can be assumed that the solid solution structure partial recrystallization occurs in this temperature range. Note that all the samples under study have a pronounced photosensitivity to visible and near-IR radiation.

A further temperature increase (up to 450–500 K) is accompanied by an abrupt resistance decrease by more than three orders of magnitude. In this case, the other electrophysical properties of the films also transform, the photoresponse disappears, and the Hall mobility sharply declines. The revealed effect is due to the decomposition beginning at $T > 450$ K of supersaturated solid solutions (B1 structure) with

separating the individual $B3$ cadmium sulfide phase from the $\text{Cd}_x\text{Pb}_{1-x}\text{S}$ crystal lattice.

The degradation of the supersaturated solid solution generally ends at $T \approx 600\text{--}650$ K. The film becomes two-phase, its residual resistance increases (a conductivity decreases) due to additional scattering of electrons at phase boundaries in accordance with Nordheim's rule. In the range $650\text{--}750$ K the observed resistance increase by about an order of magnitude is a consequence of the oxidation process, first of all, of lead sulfide to the formation of oxygenated phases (PbO , PbSO_4) [18].

For comparison, Fig. 3 shows SEM images of as-deposited films of solid solutions $\text{Cd}_{0.02}\text{Pb}_{0.98}\text{S}$ (a) and $\text{Cd}_{0.04}\text{Pb}_{0.96}\text{S}$ (c) and SEM images of these films after heating in air to 893 K (b) and (d), respectively. It should be noted that the as-deposited films morphology is approximately the same. They are different only in the sizes of crystallites formed their surface: $0.4\text{--}0.6$ μm for $\text{Cd}_{0.02}\text{Pb}_{0.98}\text{S}$ and $0.4\text{--}0.8$ μm for $\text{Cd}_{0.04}\text{Pb}_{0.96}\text{S}$. The annealing $\text{Cd}_{0.02}\text{Pb}_{0.98}\text{S}$ film consists mainly of $5\text{--}12$ μm globules, formed by smaller spherical particles ($\sim 0.50\text{--}1.0$ μm). Single $\sim 1\text{--}2$ μm crystallites are observed on its surface.

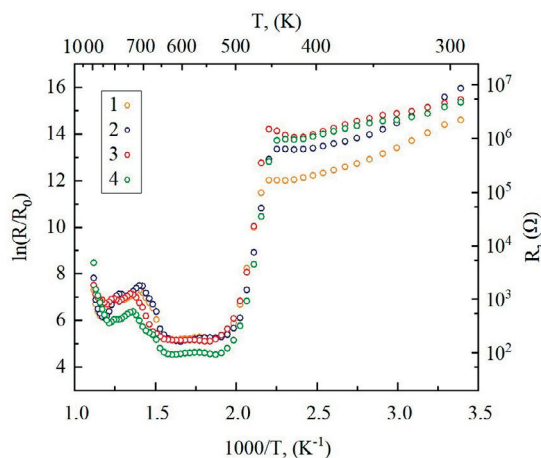


Fig. 2. The resistance dependence of $\text{Cd}_{0.02}\text{Pb}_{0.98}\text{S}$ (1), $\text{Cd}_{0.03}\text{Pb}_{0.97}\text{S}$ (2), $\text{Cd}_{0.04}\text{Pb}_{0.96}\text{S}$ (3), $\text{Cd}_{0.05}\text{Pb}_{0.95}\text{S}$ (4) solid solutions films on the heating temperature in air

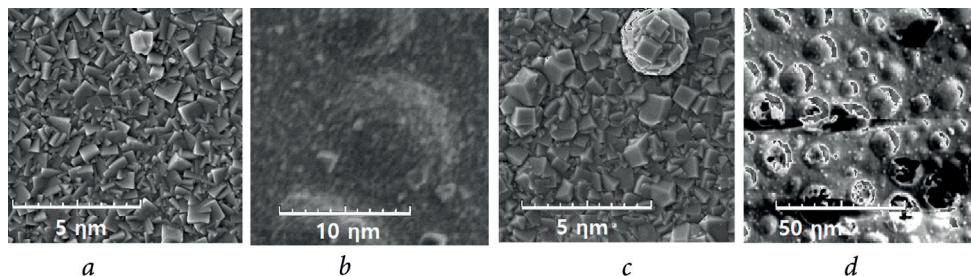


Fig. 3. SEM images of $\text{Cd}_{0.02}\text{Pb}_{0.98}\text{S}$ (a, b) and $\text{Cd}_{0.04}\text{Pb}_{0.96}\text{S}$ (c, d) solid solutions films before (a, c) and after annealing at 893 K in air (b, d). SEM images of as-deposited layers were obtained using a MIRA 3 LMU scanning electron microscope at an electron beam accelerating voltage of 10 kV, and ones after annealing were received using a Vega II SBU scanning electron microscope (Tescan, Czech Republic) at an electron beam accelerating voltage of 20 kV

The $\text{Cd}_{0.04}\text{Pb}_{0.96}\text{S}$ film globules with sizes from 4 to 20 μm are destroyed after heating to 893 K under the temperature and an increasing internal stresses. For example, structure of the film at the Fig. 3*d* exhibits strongly deformed spherical particles or globules with broken edges.

As already noted [12, 13], annealing of chemically deposited films even at 200 °C leads to the appearance of internal mechanical stresses. Therefore, in this work, we performed a quantitative assessment of the elastic mechanical stresses arising during annealing at the “ $\text{Cd}_x\text{Pb}_{1-x}\text{S}$ film — substrate” interface according to Eq. (1).

The main physical characteristics (Young’s modulus E , temperature coefficient of linear expansion TCLE α , Poisson’s ratio ν) of the $\text{Cd}_x\text{Pb}_{1-x}\text{S}$ multicomponent compound films were determined by the additive change properties rule of PbS and CdS for each composition of the solid solution [16]. The values of physical characteristics for $\text{Cd}_x\text{Pb}_{1-x}\text{S}$ solid solutions films and individual lead and cadmium sulfides with the indication of their thickness are given in Table 1.

As noted by many researchers, TCLE differences between the film and the sub-

strate plays decisive role in the occurrence of mechanical stresses in such systems. Note that the temperature expansion coefficients values for the synthesized compounds (Table 1) change insignificantly: from $18.2 \cdot 10^{-6} \text{ K}^{-1}$ to $18.7 \cdot 10^{-6} \text{ K}^{-1}$. The TCLE of the sital substrate is $5.0 \cdot 10^{-6} \text{ K}^{-1}$, and its thickness is 0.51 mm that are used for mechanical stresses calculating arising at the “film — substrate” interface.

Fig. 4 plots a quantitative estimate of elastic mechanical stresses at the “ $\text{Cd}_x\text{Pb}_{1-x}\text{S}$ solid solution film — sital substrate” interface for the temperature range 300–900 K. The calculation have taken into account the composition x and the layer thickness h . The thickness altered from 690 to 920 nm. For comparison, the figure also shows the temperature dependences of mechanical stresses arising in individual sulfides PbS and CdS.

As seen from Fig. 4, mechanical stresses in the discussion films increase with increasing temperature. Nevertheless, the CdS film does not practically has the mechanical stresses at 350–400 K temperature range. And upon reaching 900 K, insignificant expansion stresses 100 kN/ m^2 are established. The reason of this fact is practically equal the TCLE of substrate

Table 1

Young’s modulus E , linear thermal expansion coefficient α , Poisson’s ratio ν , thickness h of PbS, CdS and $\text{Cd}_x\text{Pb}_{1-x}\text{S}$ solid solution films

Parameter	Film					
	PbS	$\text{Cd}_{0.02}\text{Pb}_{0.98}\text{S}$	$\text{Cd}_{0.03}\text{Pb}_{0.97}\text{S}$	$\text{Cd}_{0.04}\text{Pb}_{0.96}\text{S}$	$\text{Cd}_{0.05}\text{Pb}_{0.95}\text{S}$	CdS
Young’s modulus, E 10^{-10} , Pa	7.02	6.96	6.94	6.91	6.88	4.20
Linear thermal expansion coefficient, $\alpha \cdot 10^6$, K^{-1}	19.0	18.7	18.5	18.3	18.2	2.5
Poisson’s ratio, ν	0.280	0.282	0.283	0.284	0.285	0.380
Films thickness, h , nm	400	740	690	920	870	360

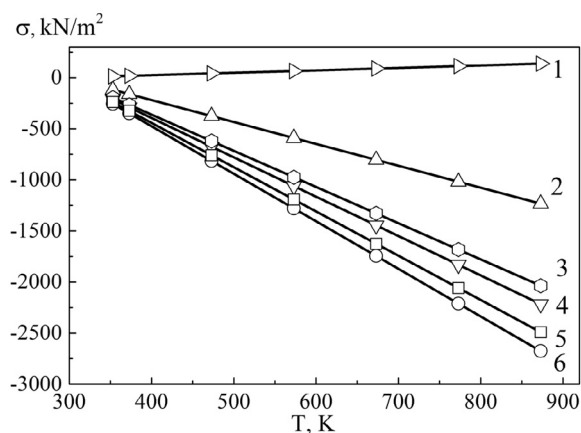


Fig. 4. Elastic mechanical stresses dependence in the systems “film — sittal substrate” on the annealing temperature in air for CdS(1), PbS (2), Cd_{0.03}Pb_{0.97}S (3), Cd_{0.02}Pb_{0.98}S (4), Cd_{0.05}Pb_{0.95}S (5), Cd_{0.04}Pb_{0.96}S (6) films

and of cadmium sulfide (TCLE of substrate is only 1.25 times greater than CdS TCLE).

As for the film of individual lead sulfide and solid solutions films based on PbS, elastic compressive stresses are created in them, that evidenced by the negative temperature dependences $\sigma = f(T)$ in Fig. 4.

The absolute value of mechanical stresses of these films increases with an increasing the annealing temperature from 350 to 893 K. Compressive stresses rise in absolute terms from about 200 to 1200 kN/m² for PbS and from 150–250 to 2000–2750 kN/m² for Cd_xPb_{1-x}S under these conditions. The ambiguous change of this characteristic with the composition of the solid solution requires attention. It would seem that the mechanical compressive stresses of the Cd_xPb_{1-x}S films should be lower with a cadmium content increasing due to their partial compensation

by the expansion stresses (the contribution of CdS). However, a more pronounce compressive stresses growth is observed in the film of the Cd_{0.02}Pb_{0.98}S solid solution (4) compared with Cd_{0.04}Pb_{0.96}S (6). The reason of that case may be larger layer thickness of film with the CdS content $x = 0.04$ (920 nm vs 740 nm). This is probably why crystallites just melted with the formation of globules in the Cd_{0.02}Pb_{0.98}S layer at 893 K (Fig. 3b), while there was a radical destruction of similar globular formations in the Cd_{0.04}Pb_{0.96}S film (Fig. 3d). The increasing layer thickness by a factor of 1.25 led the rise of internal mechanical stresses by 1.5 times. The same effect of the deposited film thickness on the magnitude of mechanical stresses was discovered for zinc selenide [14]. The strong cracking of the ZnSe film occurred due to compressive stresses at the site of globules adhesion formed it.

Conclusions

We determined the upper temperature stability limit of chemically deposited films of Cd_xPb_{1-x}S. It is in the range of 405–410 K

for CdS content (x) in supersaturated solid solutions equal to 0.06, 0.122 and 0.176, and about 450 K for x from 0.02 to 0.05, re-

spectively. Solid solutions decompose into two phases at higher temperatures: a solid solution with the equilibrium cadmium sulfide content at the given temperature and X-ray amorphous CdS. The quantitative assessment of internal mechanical stresses caused by annealing of $\text{Cd}_x\text{Pb}_{1-x}\text{S}$ films was carried out for the first time ever

in the range of 300–900 K. It is shown that the mechanical stresses at the “ $\text{Cd}_x\text{Pb}_{1-x}\text{S}$ film — siall substrate” interface increase with annealing temperature. Thus, the compressive stresses under these conditions increase in absolute terms from 150–250 to 2000–2750 kN/m² depending on the composition of the solid solution.

Acknowledgements

The research was supported by RFBR, projects No. 20-48-660041r_a and No. 18-29-11051mk, and was carried out within the state assignment of Ministry of Science and Higher Education of the Russian Federation (theme No. H687.42B.223/20).

References

1. Nichols PL, Liu Z, Yin L, Turkdogan S, Fan F, Ning CZ. $\text{Cd}_x\text{Pb}_{1-x}\text{S}$ Alloy Nanowires and Heterostructures with Simultaneous Emission in Mid-Infrared and Visible Wavelengths. *Nano Lett.* 2015;15:909–16.
doi:10.1021/nl503640x
2. Ahmada SM, Kasima SJ, Latif LA. Effects of thermal annealing on structural and optical properties of nanocrystalline $\text{Cd}_x\text{Pb}_{1-x}\text{S}$ thin films prepared by CBD. *Jordan Journal of Pharmaceutical Sciences.* 2016; 9:113–22.
3. Zarubin IV, Markov VF, Maskaeva LN, Zarubina NV, Kuznetsov MV. Chemical sensors based on a hydrochemically deposited lead sulfide film for the determination of lead in aqueous solutions. *J Anal Chem.* 2017;72:327–32.
doi:10.1134/S1061934817030145
4. Bezdetnova AE, Markov VF, Maskaeva LN, Shashmurin YuG, Frants AS, Vinogradova TV. Determination of nitrogen dioxide by thin-film chemical sensors based on $\text{Cd}_x\text{Pb}_{1-x}\text{S}$. *J Anal Chem.* 2019;74:1256–62.
doi:10.1134/S1061934819120025
5. Hernadez-Borja J, Vorobiev YV, Ramirez-Bon R. Thin film solar cells of CdS/PbS chemically deposited by an ammonia-free process. *Solar Energy Materials and Solar Cells.* 2011;95:1882–8.
doi:10.1016/j.solmat.2011.02.012
6. Obaid AS, Mahdi MA, Hasson Z., Bououdina M. Preparation of chemically deposited thin films of CdS/PbS solar cell. *Superlattice Microst.* 2012;52:816–23.
doi:10.1016/j.spmi.2012.06.024
7. Barote MA, Kamble SS, Yadav AA, Suryavanshi RV, Deshmukh LP, Masumdar EU. Thickness dependence of $\text{Cd}_{0.825}\text{Pb}_{0.175}\text{S}$ thin film properties. *Materials Letters.* 2012;78:113–5.
doi:10.1016/j.matlet.2012.03.018
8. Maskaeva LN, Markov VF, Porkhachev MYu, Mokrousova OA. Termicheskaya i radiatsionnaya ustoychivost' IK-detektorov na osnove plenok tverdykh rastvorov $\text{Cd}_x\text{Pb}_{1-x}\text{S}$ [Thermal and radiation stability ir-detectors based on films of solid solu-

- tions $\text{Cd}_x\text{Pb}_{1-x}\text{S}$]. Pozharovzrybezopasnost [Fire and Explosion Safety]. 2015;24:67–73. Russian.
doi:10.18322/PVB.2015.24.09.67–73
9. Markov VF, Maskaeva LN, Ivanov PN. Gidrokhimicheskoe osazhdenie plenok sulfidov metallov: modelirovanie i eksperiment [Chemical bath deposition of metal sulfide films: modelling and experiment]. Yekaterinburg: Ural Branch of RAS; 2006. 218 p. Russian.
 10. Gardi SB, Singh A, Yousuf M. Structural stability of PbS films as function of temperature. Thin Solid Films. 2003;431:506–10.
doi:10.1016/S0040-6090(03)00245-1
 11. Shugurov AR, Panin AV. Mechanisms of periodic deformation of the film — substrate system under compressive stresses. Physical Mesomechanics. 2009;13:79–87.
doi:10.1016/j.physme.2010.03.010
 12. Krylov PN, Romanov EA, Fedotova IV. Thermal annealing influence on the zinc sulfide nanocrystalline films structure. Semiconductors. 2011;45:125–9.
doi:10.1134/S1063782611010131
 13. Krylov PN, Romanov EA, Fedotova IV. Struktura i svoystva nanokristallicheskich plenok sulfida i selenida tsinka [Structure and properties of nanocrystalline films of zinc sulfide and selenide]. [Surface. X-ray, synchrotron, and neutron studies]. 2013;5:65–9. Russian.
doi:10.7868/s0207352813050065
 14. Maskaeva LN, Markov VF, Fedorova EA, Kuznetsov MV. Influence of the conditions of the chemical bath deposition of thin ZnSe films on their morphology and internal mechanical stresses. Russian Journal of Applied Chemistry. 2018;91:1528–37.
doi:10.1134/S1070427218090161
 15. Maskaeva LN, Pozdin AV, Markov VF, Voronin VI. Influence of the substrate nature on the composition CdPbS films and mechanical stresses on the “film — substrate” interface. Semiconductors. 2020;12:1310–9.
doi:10.21883/FTP.2020.12.50230.9506
 16. Kasimov D, Lyutfalibekova AE. Raschet uprugikh mekhanicheskikh napryazheniy v neodnorodnykh poluprovodnikovyykh strukturakh [Calculation of elastic mechanical stresses in inhomogeneous semiconductor structures]. Tekhnologiya i konstruirovanie v elektronnoy apparature [Technology and design in electronic equipment]. 2002;2:13–14. Russian.
 17. Shelimova LE, Tomashik VN, Grytsiv VI. Diagrammy sostoyaniya v poluprovodnikovom materialovedenii : (sistemy na osnove khal'kogenidov Si, Ge, Sn, Pb) [State diagrams in semiconductor materials science : (systems based on Si, Ge, Sn, Pb chalcogenides)]. Moscow: Nauka; 1991. 368 p. Russian.
 18. Kitaev GA, Protasova LG, Kosenko VG, Markov VF. Oxidation of chemically precipitated lead sulfide. Inorganic Materials. 1993;29:2017–8.
 19. Marvin JW. Handbook of Laser Science and Technology. CRC Press LLC; 2003. 499 p.